Regional Environmental Change (2022) 22:112
https://doi.org/10.1007/s10113-022-01957-5

ORIGINAL ARTICLE

Assessing observed and projected flood vulnerability under climate change using multi-modeling statistical approaches in the Ouémé River Basin, Benin (West Africa)

Jean Hounkpè[1] · Djigbo F. Badou[1,2] · D. M. Maurice Ahouansou[3] · Edmond Totin[4] · Luc O. C. Sintondji[1]

Received: 14 December 2020 / Accepted: 12 July 2022 / Published online: 6 September 2022

Abstract
Climate change has severe impacts on the livelihoods of West-African communities with the floods of the late 2000s and early 2010s serving as factual evidence. Focusing on the assessment of observed and future vulnerability to extreme rainfall in the tropical Ouémé River Basin, this study aims to provide scientific evidence to inform national adaptation plans. Observed climate variables, historical and future outputs from regional climate models, topographic, land cover, and socioeconomic data were used in the vulnerability assessment. This assessment was based on four indicator normalization methods (min–max, z-scores, distance to target, and ranking), two aggregation techniques (linear and geometric), four classification methods (quantile, standard deviation, equal intervals, natural breaks), and three robustness evaluation approaches (spearman correlation, Akaike Information Criterion (AIC), and average shift in ranks). Based on the AIC, it was found that "equal intervals" is the overall best classification method and the min–max normalization with linear aggregation (MM.LA) outperformed other methods. The median scenario indicates that the population of the Ouémé Basin is vulnerable to the adverse impacts of climate change for the historical (1970–2015) and future periods (2020–2050) as a result of low adaptive capacity. By 2050, the southern part of the Ouémé Basin will be highly vulnerable to pluvial flooding under RCP 4.5. Vulnerable municipalities will continue to suffer from flooding if adequate adaptation measures including water control infrastructure (development and expansion of rainwater and wastewater drainage systems) and appropriate early warning systems to strengthen community members' resilience are not taken.

Keywords Pluvial floods · Vulnerability assessment · Multiple methodological approaches · Ouémé Basin · Benin

Introduction

Flood is among the most devastating natural disasters affecting human beings and natural ecosystems. According to Sultan and Gaetani (2016), West Africa is one of the most exposed regions to the adverse effects of climate change. While the 1970s and 1980s were marked by the

Communicated by Stefan Liersch and accepted by Topical Collection Chief Editor Christopher Reyer.

This article is part of the Topical Collection on *Climate Change Adaptation, Resilience and Mitigation Challenges in African Agriculture*.

✉ Jean Hounkpè
jeanhounkpe@gmail.com

Djigbo F. Badou
fdbadou@gmail.com

D. M. Maurice Ahouansou
maurice.ahouansou@fsa.uac.bj

Edmond Totin
edmond.totin@gmail.com

Luc O. C. Sintondji
o_sintondji@yahoo.fr

[1] Institut National de l'Eau, Université d'Abomey Calavi, Abomey Calavi, BP 2008, Benin

[2] Ecole d'Horticulture Et d'Aménagement Des Espaces Verts, Université Nationale d'Agriculture, BP43 Kétou, Bénin

[3] Faculté des Sciences Agronomiques, Université d'Abomey Calavi, Abomey Calavi, Benin

[4] Ecole de Foresterie Tropicale, Université Nationale d'Agriculture du Benin, BP 43, Kétou, Benin

great drought (Nicholson 2001; Lebel and Ali 2009), which negatively impacted the region's economy, the 2000s recorded unprecedented floods. The annual average of flood events has increased from less than 5 to 11 between 1966 and 2020 (EM-DAT 2022) in West Africa, likely due to the increase in heavy rainfall frequency and intensity in the region (Nkrumah et al. 2019; Tazen et al. 2019). In Benin, between 1984 and 2010, floods caused the death of 71 persons and injured an average of 279,971 people per year (MEHU, 2011). The worst happened in 2010 when the country experienced the most devastating floods in its history, resulting in the death of 46 people and an estimated loss of 80,778,431 US dollars (World Bank 2011). Recent years also recorded extreme flood events. The year 2020 was a dreadful one as high flows led to the death of 29 persons and affected 6869 people in northern Benin (e.g., in Kandi, Karimama, and Malanville).

Evaluating flood vulnerability is relevant to inform the design of integrated flood risk management. Flood vulnerability can be understood as the degree to which a system is likely to be harmed by water under various factors, including exposure, sensitivity, and adaptive capacity (Parry et al. 2007) as discussed in the "Index of flood vulnerability components" section below. There is a wide range of studies that have evaluated flood vulnerability in the context of climate change through different approaches, including damage evaluation approach (Tóth 2008), socioeconomic and biophysical vulnerability indicators (Hebb and Mortsch 2007; Birkmann et al., 2022), integrated vulnerability index (Kumpulainen 2006), coastal city flood vulnerability index (Balica et al. 2012), and GIS-based method (Coto, 2002). Areas experiencing high flood risk lack sufficient water drainage infrastructures.

In Benin, there are limited studies on flood vulnerability assessment. Behanzin et al. (2016) conducted a GIS-based mapping of flood vulnerability and risk in the Niger River Valley. The study highlighted some flood vulnerability drivers including poverty rates and socioeconomic factors. In the Ouémé River Basin (ORB), previous studies have documented the exposure of flood vulnerability focusing on extreme rainfall trends (Attogouinon et al. 2017; N'Tcha M'Po et al. 2017), stationary flood frequency analysis, non-stationary flood frequency analysis (Hounkpè et al. 2015b, 2015a), the impact of land use change on floods (Hounkpè et al. 2019), and hydrological modeling of flooding. Apart from the assessment of exposure to flood events, there is a huge gap in the literature on flood vulnerability as defined above over the ORB. This study, the very first of its kind in Benin, assesses specifically observed and projected flood vulnerability in the ORB using multi-modeling statistical approaches. The multi-modeling approaches imply the use of two or more methods at each stage of flood vulnerability assessment as recommended in the literature (Feizizadeh and Kienberger 2017; Nazeer and Bork 2019, 2021; Moreira et al. 2021).

Methodological approach

Study area

The Ouémé River is 548 km long and drains about 49,256 km^2 at its main outlet of Bonou (Deng, 2007). With its source located in Kpabégou, about 10 km from Djougou in northwestern Benin, the river flows from North to South and is joined by its main tributaries, the Okpara (200 km) on the left bank and the Zou (150 km) on the right bank. The ORB is located between latitudes of 10°09′33″N and 6°20′14″ N and longitudes 1°30′E and 2°30′E (Fig. 1) and is relatively flat.

The ORB is composed of three climatic zones based on the rainfall regime (Deng 2007): (i) the unimodal rainfall regime of the northern part of the basin comprising two seasons, the rainy season that falls between May and October and the dry season that spans from December to April; (ii) the bimodal rainfall regime of the southern part of the basin with two wet seasons, a long season between March and July and a short season between September and mid-November and a long dry season between November and March; and (iii) the transition rainfall regime in the center of the basin, a rainy season between March and October, with or without a short dry season in August. The average annual rainfall ranges between 1100 mm in the north (Deng 2007; Badou et al. 2015) and 1340 mm in the South of the basin. As a result, precipitation decreases northwards and results in a steep gradient. The average annual temperatures fluctuate between 26° and 30 °C (Bossa et al. 2014). The 1970–2015 period was chosen to assess the current vulnerability as it covers the recent trends observed in the climatic variable across West Africa (Badou et al. 2017), while the 2020–2050 period was chosen to assess the mid-century future vulnerability. The future period started in 2020 as the initial work was done before 2020.

Index of flood vulnerability components

In this paper, the concept of vulnerability as defined in the AR4 is used which is nearly equivalent to the actual risk concept (AR5). The vulnerability is therefore defined as the "degree to which a system is susceptible to and unable to cope with, adverse effects of climate change, including climate variability and extremes" (Solomon et al., 2007; Page 6). The vulnerability framework (see supplementary materials) was adopted from Fritzsche et al. (2014). This framework was initially developed by Füssel and Klein (2006) and was further used by Lung et al. (2013) for a multi-hazard

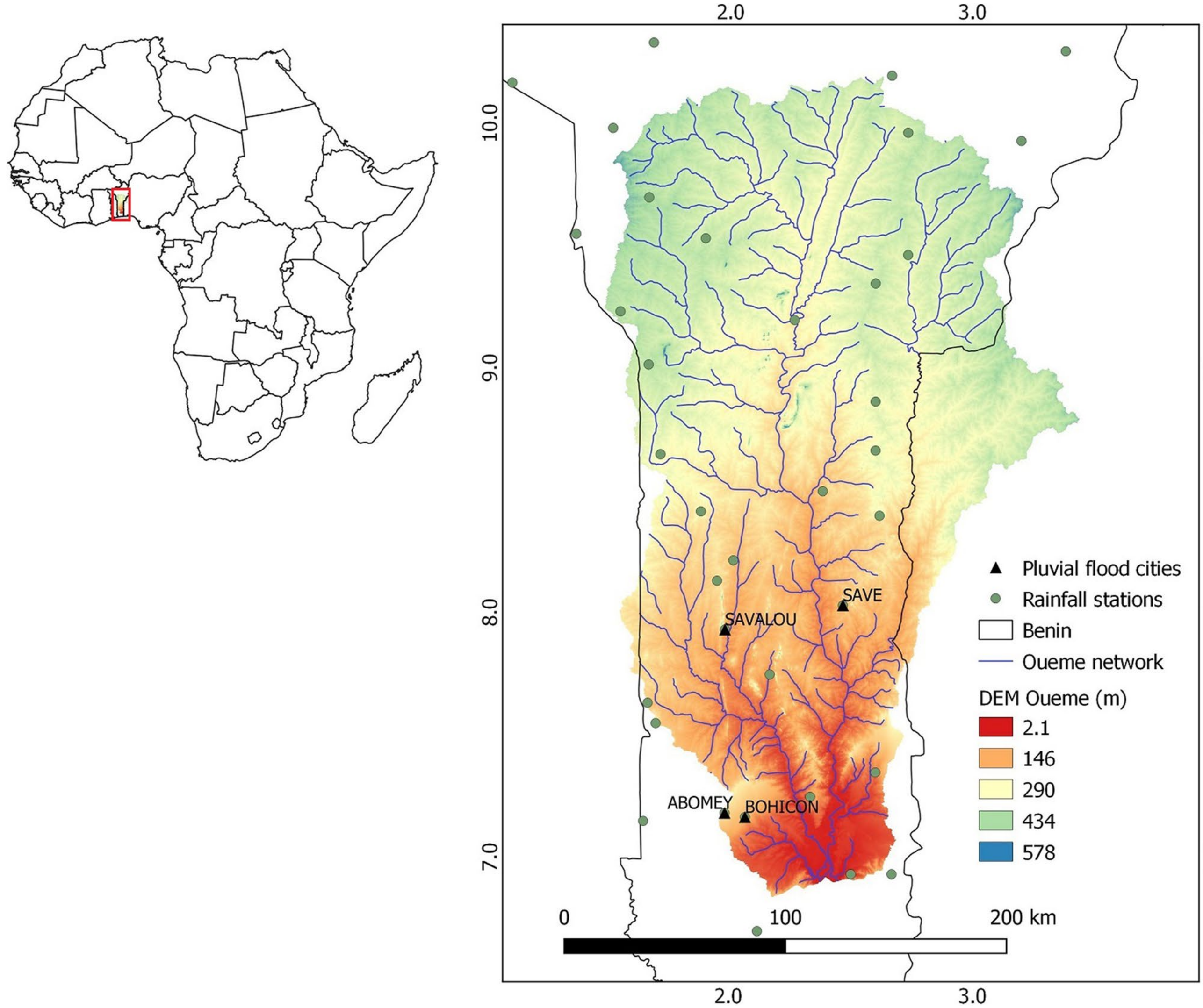

Fig. 1 Location of the Ouémé River Basin in Africa and Benin as well as the rainfall stations

regional level impact assessment for Europe combining indicators of climatic and non-climatic change. The current work was done using the same conceptual framework:

$$Vulnerability = f(Exposure,\ Sensitivity,\ Adaptation\ Capacity)$$

The methodological framework adopted for the flood vulnerability assessment is synthesized in Fig. 2. It is based on four indicator normalization methods, two aggregation techniques, four classification methods, and three robustness evaluation approaches. Each of the components of this framework is described in the following lines.

Identification of flood vulnerability indicators

The impact chain of key factors considered for shaping current and future flood vulnerability in the ORB was elaborated following Fritzsche et al. (2014) (see figure F1 in supplementary materials). Relevant indicators are selected to assess each of the components of the impact chain. For example, poverty, the existence and effectiveness of flood early warning systems, and access to information are the indicators chosen for the assessment of the adaptation capacity component. Indicators are used to characterize factors. For example, the availability of climate information (weather stations) is selected as an indicator to characterize the factor "access to information." Municipalities are the basic geographical unit level considered for the analysis. The ORB has a total of thirty-four (34) municipalities.

Flood exposure or climate impact-drivers In Benin, the majority of floodings are caused by torrential rains making precipitations the main cause of flooding in the ORB (MEHU 2011). Therefore, in this study, rainfall was

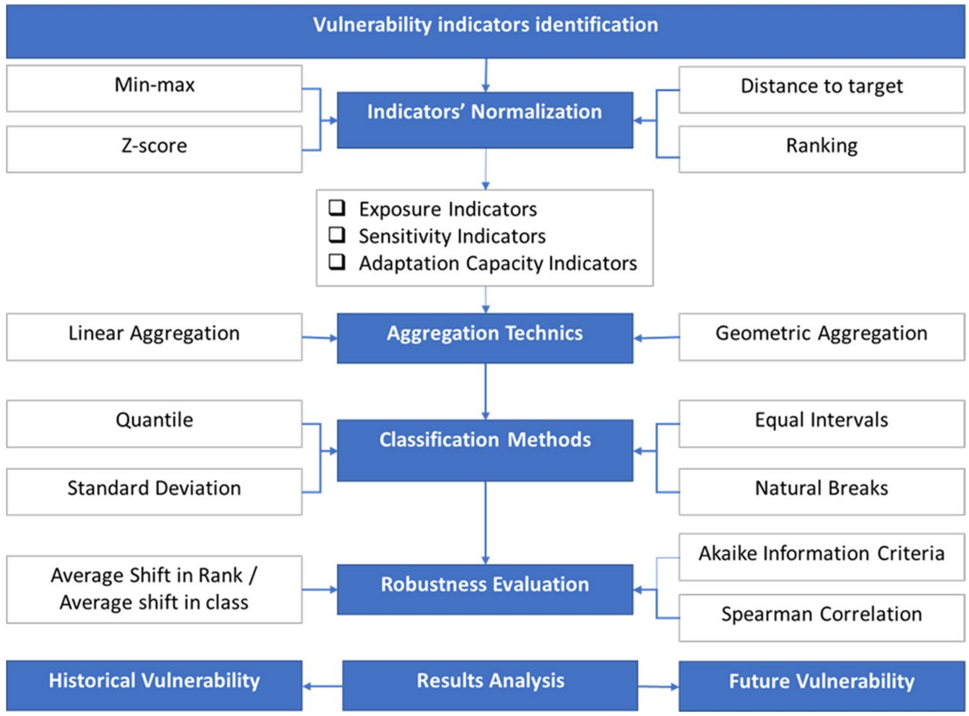

Fig. 2 Methodological framework for flood vulnerability analysis

purposely used as the key factor for exposure analysis. Based on the analysis of rainfall data and natural factors (topography and soil), SAP-Benin (2015) determined warning level thresholds associated with flooding for cities prone to pluvial flooding. Four alert levels were identified, and thresholds slightly vary with the considered station. For consistency purposes, the same thresholds were used for all the stations of the ORB. The indicators considered are (i) average annual number of rainy days greater than or equal to 60 mm, (ii) average annual number of rainy days between 60 and 90 mm, (iii) average annual number of rainy days between 90 et 110 mm, and (iv) average annual number of rainy days greater than or equal to 110 mm. For each station, the number of rainy days was determined according to these thresholds. This resulted in a three-time series of each station's number of rainy days. For pluvial flood studies, sub-daily data resolution should be preferred as rainfall-induced floods could occur in a few hours. However, due to the paucity of higher temporal resolution data, daily data was considered. In addition, the outputs of the RCMs used are provided at a minimum temporal resolution of a day.

Flood sensitivity Topography (slope index) and land use substantially influence the velocity of water flow and have therefore been selected as drivers of sensitivity. The land use unit's susceptibility to favor flooding was considered to scale the land use unit from 1 to 5 (see table T1, supplementary materials). For instance, urban areas are prone to flooding while forests are not. Similarly, the slope is one of the influencing factors of flooding. The same applies to population density. The sensitivity of a population to flood is directly linked to its density. Other things being equal, a population with a higher density is more subject to flooding than one with a lower density.

Flood adaptation capacity Adaptation capacity is a set of mechanisms and actions to cope with the risks of flooding. The indicators of monetary wealth (INSAE 2015), the availability of a contingency plan/civil protection committee at the municipality level, and the availability of hydro-climatic information were considered to assess the adaptation capacity to flooding in the ORB.

Standardization of indicators

Given the plurality of the drivers considered in this study, it was necessary to standardize them for comparison and interpretation purposes. The normalization was based on four methods (Yoon 2012; Hudliková 2013; Moreira et al. 2021) namely the Min–max, z-score, distance to target and ranking with X_i the ith element of the indicator X, and NI_i the standardized value of X_i.

– The min–max method standardized the indicator (X) to the scale between zero, corresponding to the lower indicator value and 1 corresponding to the highest indicator value using the following formula:

$$NI_i = \frac{X_i - min(X)}{max(X) - min(X)}$$

– The z-score standardized the indicators to a new variable with a mean value of zero and a standard deviation of 1. It is based on the following formula where $\underline{X}$ and σ_X are respectively the mean and standard deviation of X:

$$NI_i = \frac{X_i - \underline{X}}{\sigma_X}$$

– The distance to target method normalizes indicators by dividing the unit's value by a reference target (i.e., maximum value):

$$NI_i = \frac{X_i}{max(X)}$$

– The ranking approach attributes to each indicator value its ordinary rank in the series:

$$NI_i = rank(X_i)$$

Weighting scheme

No weighting scheme was considered in this study to avoid subjectivity in choosing the weight as indicated by Nazeer and Bork (2021), Villordon (2012), and Moreira et al. (2021). It was assumed that all the initial indicators contribute equally to flood vulnerability. Therefore, the same weight was applied to all normalized indicators during the aggregation stage.

Aggregation of indicators and vulnerability classification approaches

After the normalization, the next step was to group components (exposure, sensitivity, and adaptation capacity). It was assumed that the average values of the indicators under each component following the municipalities were representative of the component in line with the no different weighting scheme previously indicated. The vulnerability was inferred by combining the exposure, sensitivity, and adaptation capacity. Exposure and sensitivity on the one hand and adaptation capacity on the other hand have a contrary effect on vulnerability. An increase in exposure and/or sensitivity increases vulnerability, while an increase in adaptive capacity reduces vulnerability. The aggregation of the exposure (EP), sensitivity (SE), and adaptation capacity (AC) into vulnerability index (VI) were done using the linear and the geometric approaches as follow:

– The linear aggregation approach was based on the vulnerability assessment method as defined by Ritzsche et al. (2015):

$$VI = \frac{\frac{(EP+SE)}{2} + [1 - AC]}{2}$$

– The geometric aggregation was performed using the formula below:

$$VI = \frac{SE * EP}{AC}$$

To account for uncertainties due to the classification of the vulnerability indexes, four classification methods (quantile, standard deviation, equal intervals, and natural breaks) (Moreira et al. 2021) were considered, and vulnerability indexes were grouped into five classes (very low, low, medium, high, and very high). Differences in the classification methods were evaluated using visual inspection and numerical criteria.

Robustness and sensitivity evaluation

Three metrics were considered for assessing the robustness and sensitivity of composite indicators (vulnerability indexes). These are:

(i). Spearman correlation coefficient (Spearman 1904; Hauke and Kossowski 2011; Nazeer and Bork 2019): Spearman correlation coefficient is a nonparametric measure of the strength and direction of existing association between two quantitative variables. It was used to evaluate the relationship between any couple of model participant scenarios.

(ii). Average absolute shift in rank (OECD 2005; Saisana et al. 2005; Nazeer and Bork 2021): Average absolute shift in rank ($\underline{R}s$) is computed as the average of the absolute difference between the municipalities' rank and a reference value such as the median rank of all scenarios. Its formula is as follows with Y_{MR}, the median rank; Y_i, the rank derived through different scenarios for a given Y municipality across the 34 municipalities ($i = 1, 2, .., 34$):

$$\underline{R}s = \frac{1}{34}\sum_{i=1}^{34}(Y_{MR} - Y_i)$$

(iii). Akaike information criterion (Akaike 1974): this criterion is used for evaluating how well a model fits the data it was generated from. For more information on the use of this criterion in vulnerability assessment, the reader can refer to Mazari et al. (2017) and Moreira et al. (2021)

Scenario analysis

The combination of the various normalization methods (min–max, z-scores, distance to target, and ranking) (Moreira et al. 2021), aggregation techniques (linear and geometric), and classification approaches (quantile, standard deviation, equal intervals, natural breaks) led to the realization of 24 participating members. The geometric aggregation capability to treat information derived from min–max and distance to target is limited (Garg et al. 2018) and these combinations were excluded as these two normalization techniques transform the minimum value into zero and thus produce a final zero vulnerability. The vulnerability indexes were generated using the four normalization techniques namely the Z-score (ZC), the min–max (MM), the distance to target (DT), and ranking (RA), combined with two aggregations methods namely the geometric aggregation (GA) and the linear aggregation (LA) and led to six vulnerability indexes (ZC.GA, ZC.LA, MM.LA, DT.LA, RA.LA, RA.GA) referred here as scenarios. ZC.GA corresponds to Z-score normalization technique combined with the geometric aggregation method for flood vulnerability index calculation. ZC.LA, MM.LA, DT.LA, RA.LA, and RA.GA should be similarly interpreted.

The observed and projected vulnerability was assessed based on the indicators presented above. The difference between these two types of vulnerability is mainly at the exposure level. For the historical vulnerability, exposure was assessed using both ground climate station data and regional climate models (RCMs) outputs (downscaled and bias corrected) over the period 1970–2015, whereas, for future vulnerability, data from the same RCMs (REMO/MPIESM, RCA4/IPSL, CCLM4/HADGEM2, RACMO/ECEARTH) downscaled and bias corrected were used to assess the exposure over the 2020–2050 period. The intermediate scenario RCP4.5 (Representative Concentration Pathway) was used in this study. Compared to the other scenarios, it is the most plausible scenario fitting the current context (Edenhofer et al. 2012) of global climate change mitigation efforts. The scenario RCP8.5 is too pessimistic and not consistent with current climate change mitigation agendas. The model outputs were corrected via a trend-preserving bias correction technique applied to the RCM climate projections. This bias correction technique adjusts climate simulations to a reference dataset (regioclim.climateanalytics.org/choices, accessed on 10/12/2018) over a reference period without influencing projected trends (Hempel et al. 2013). Other vulnerability components were considered constant to evaluate to what extent climate change specifically impacts flood vulnerability in the study area.

Results

Influence of different normalization and aggregation approaches on flood vulnerability indexes

Relationship between flood vulnerability scenarios

The partial correlations between flood vulnerability indexes (FVI) were generated using four normalization techniques namely the Z-score (ZC), min–max (MM), distance to target (DT), and ranking (RA), combined with two aggregations methods namely the geometric aggregation (GA) and the linear aggregation (LA), and are presented in figure F2 of the supplementary material. The FVI based on Z-score and geometric aggregation (ZC.GA) exhibited a negative correlation with other vulnerability indexes suggesting a dissimilarity between ZC.GA and the other methods (Moreira et al. 2021). The Spearman correlation coefficients obtained between the remaining scenarios are very high and statistically significant at a 5% level indicating a good agreement between these scenarios. The highest correlation value of 0.98 was obtained for linear aggregation between the scenarios DT.LA and MM.LA; RA.LA and MM.LA; and MM.LA and ZC.LA while the lowest significant correlation of 0.86 was obtained between DT.LA and Geometric aggregation for ranking technique.

Robustness of flood vulnerability indexes based on $\underline{Rs}$

The robustness based on the average shift in ranking relative to the median provides a basis for uncertainty analysis of normalization and aggregation methods. Table 1a shows the average shift in rankings for the 34 municipalities indicated in Fig. 3. A value of $\underline{Rs}$ close to zero indicates a classification similar to the median ranking. The Z-score combined with the geometric aggregation (ZC.GA) indicated the highest $\underline{Rs}$ value implying a dissimilarity with the median ranking and thus high uncertainties with the vulnerability estimated based on this method (Hudrliková 2013). The linear aggregation method except for the DT.LA provided low $\underline{Rs}$ values and therefore low uncertainties in contrast to the geometric aggregation.

The relatively low values of $\underline{Rs}$ combined with the high and statistically significant correlation (at 5% level) among MM.LA, ZC.LA, and RA.LA imply that the vulnerability indexes estimated through this method will not highly affect the ranking of the municipalities as indicated by Nazeer and Bork (2019). Therefore, MM.LA, ZC.LA, and RA.LA can be used for further investigation.

Table 1 Average shift in rank (a) and performances of the classification methods for the FVI based on the different normalizations and aggregation techniques using the average shift in classes (b) and the Akaike information criterion (c). The values in bold indicate the best classification method for each scenario

	MM.LA	ZC.LA	ZC.GA	DT.LA	RA.LA	RA.GA
(a)	Average shift in rank ($\underline{Rs}$)					
Scenarios	1.19	1.13	11.75	2.04	1.10	2.72
(b)	Average shift in vulnerability classes					
Quantile	0.50	0.38	0.53	0.51	0.25	0.62
Standard deviation	*0.09*	0.88	0.26	**0.07**	0.31	0.24
Equal intervals	**0.00**	**0.15**	0.65	0.19	0.22	0.35
Natural breaks	*0.12*	0.24	**0.24**	*0.10*	**0.07**	**0.15**
(c)	Akaike information criterion (AIC)					
Quantile	110.75	-	-	117.68	3585.93	4613.80
Standard deviation	110.67	-	-	117.68	3585.93	4613.80
Equal interval	**110.66**	-	-	117.68	3585.93	4613.80
Natural breaks	110.76	-	-	117.72	**3585.57**	**4610.92**

Flood vulnerability index classification uncertainties

To evaluate the uncertainties related to the spatial repartition of the FVI, five classes of vulnerability indexes were created namely “very low,” “low,” “medium,” “high,” and “very high” using four classification methods: quantile, standard deviation, equal intervals, natural breaks (Fig. 4). Considering the linear aggregation, the min–max (MM.LA), the z-score (ZS.LA), the distance to the target (DT.LA), and the ranking (RA.LA) normalizations provide generally similar results for the quantile (Fig. 4a, b, d, e, f), standard deviation (Fig. 4g, h, j), and equal intervals (Fig. 4m, n, p) classifications respectively. The slight differences noted for the aforementioned sub-figures are the change from one class to the next, which is acceptable. Similarly, the ranking normalization with linear (RA.LA) and geometric (RA.GA) aggregations provide nearly the same spatial characteristics for quantile (e, f), standard deviation (k, l), and natural breaks (w, x) classifications.

Vulnerability results obtained from the geometric aggregation combined with the z-score (ZC.GA: c, i, o, u) and somehow with the ranking (RA.GA: l, r, x) normalizations are drastically different from their respective companion classes. For instance, a change from very low (r) to very high (c) vulnerability classes for some municipalities and vice versa was observed. Using this approach may lead to underestimating or overestimating the actual vulnerability. These results confirm previous findings obtained on the negative correlation and highest value of the average shift in rank (see Relationship between flood vulnerability scenarios and Robustness of flood vulnerability indexes based on $\underline{Rs}$) that the geometric aggregation provides diverging vulnerability outputs comparatively to other methods.

Concentrating on the variability due to the classification methods, a shift from one class to the next is noticed for all normalization and aggregation methods. However, some shifts from very low (lower left municipalities of Fig. 4b, t) to medium (lower left municipalities of Fig. 4h, n) were also found.

Beyond the visual inspection, the average shift in the five classes of vulnerability for the 34 municipalities was computed using the median classes as reference (Table 1b). Focusing on the uncertainties linked with the classification methods, the equal intervals show an average shift in the class of zero for min–max normalization and linear aggregation implying a perfect agreement with the overall median classes. Similarly, equal interval appears to be the best classification method for z-score with linear aggregation (ZC.LA). For ranking (respectively z-score) normalizations combined with geometric and linear (RA.GA, RA.LA) (respectively geometric, ZC.GA) aggregations, natural breaks were the best vulnerability classification method. The uncertainties relative to the median classes of vulnerability are the lowest for the standard deviation when considering the distance to target normalization and linear aggregation (DT.LA) of vulnerability indicators. The quantile classification did not outperform any of the other classification methods regardless of the normalization and aggregation methods considered.

The performance of the classification was further investigated using the Akaike information criterion (AIC, Table 1c). AIC was not computed for vulnerability indexes based on z-score normalization and geometric/linear aggregations (ZC.GA, ZC.LA) since the sum of the indicators is equal to zero (average value of zero for z-score). The results based on the AIC are similar to one of the average shifts in vulnerability classes. The natural breaks classification is the best for ranking normalization with linear and geometric aggregation (RA.LA, RA.GA). Equal interval classification provides the lowest value of AIC and thus is the overall best classification method for all normalization and aggregation approaches. The lowest AIC was obtained for min–max normalization with linear aggregation (MM.LA). These results imply that the

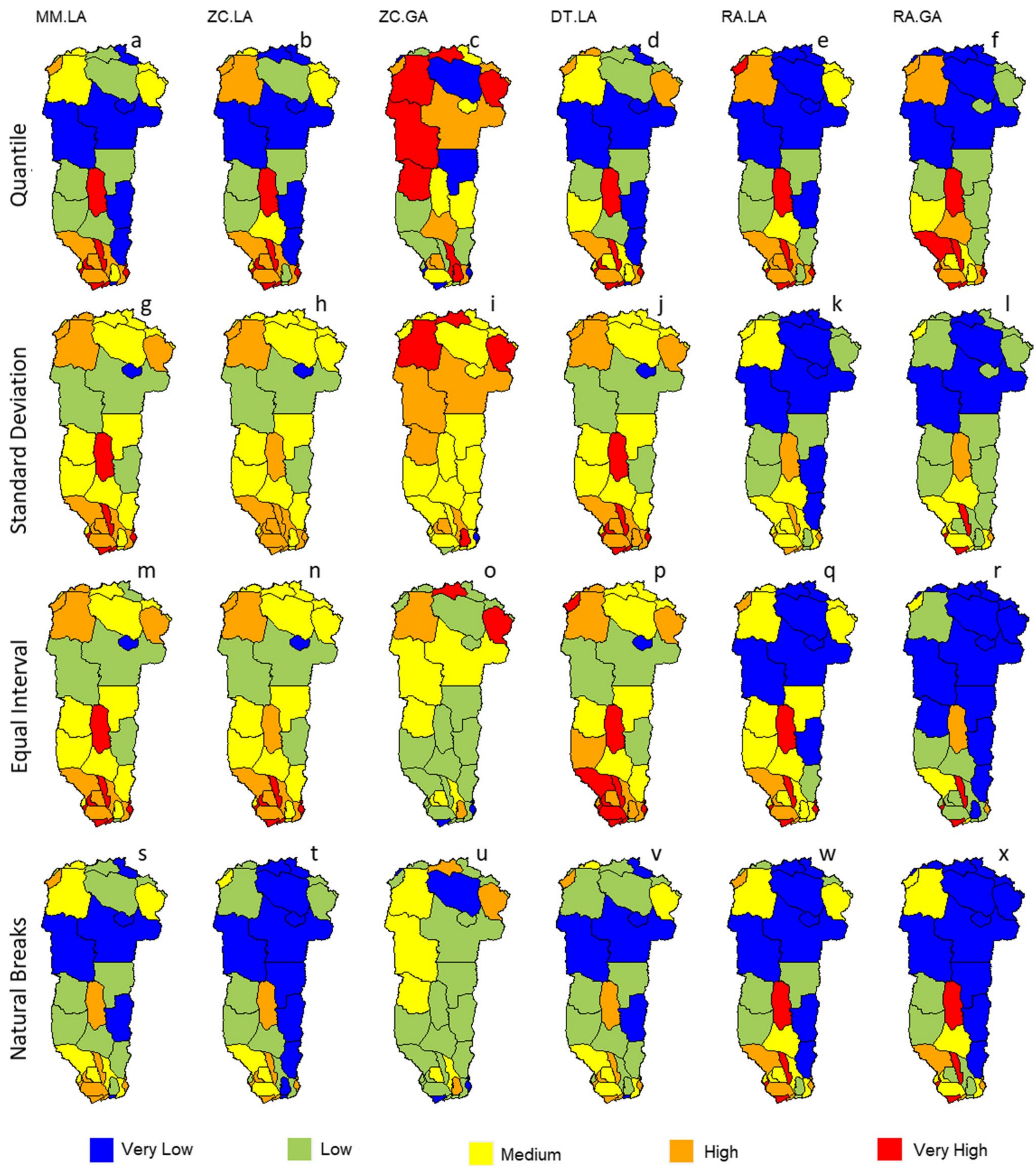

Fig. 3 Shift in vulnerability index classes using the quantile, standard deviation, equal intervals, and natural breaks classification

min–max normalization with linear aggregation (MM.LA) combined with the equal intervals classification can be used for future investigation of flood vulnerability in the Ouémé Basin.

Historical and future flood vulnerability in Ouémé River Basin

Historical flood vulnerability

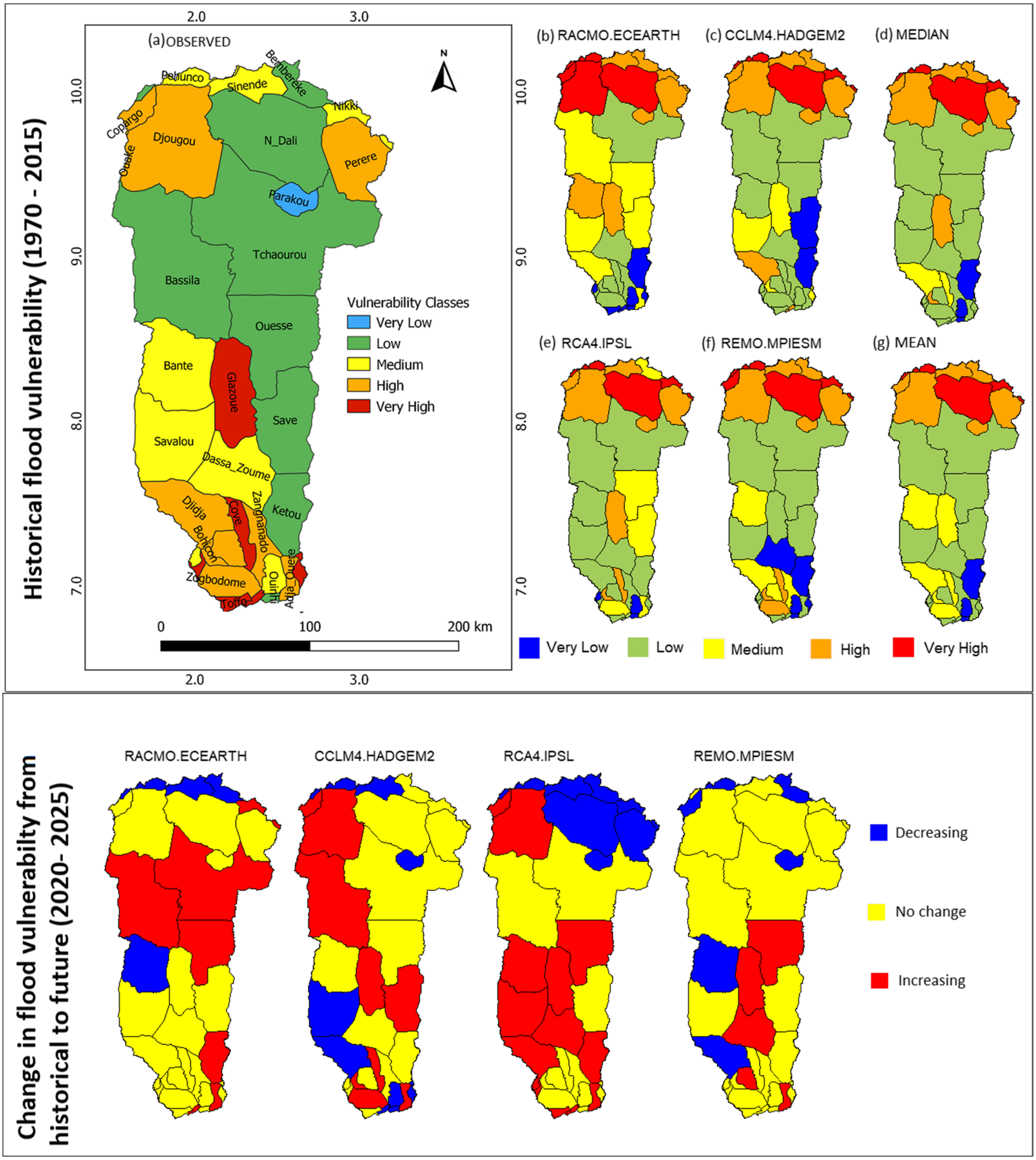

Fig. 4 Historical flood vulnerability (1970–2015) based on the median of the 24-member scenarios using observed data (**a**), simulated data for the historical period by four Regional Climate Models (RCMs; **b**, **c**, **e**, **f**), median (**d**) and mean (**g**) from the RCMs for the upper box. The lower box shows the change in the median flood vulnerability from the historical to the future period (2020–2050) based on 24 participating members for each of the four RCMs

The upper box of Fig. 4 presents the median vulnerability of the 24 participating members for the historical period based on the observed data (a) and simulated data for the four RCMs. As far as the vulnerability obtained from the observed data is concerned, the municipalities of Glazoue, Cove, Zagnanado, Agbangnizoun, Toffo, Ze, and Pobè appeared to have a very high vulnerability to climate change in the Ouémé Basin.

In addition to these municipalities, most areas in the southern part of the basin (see Fig. 5) showed a high vulnerability to pluvial flooding. In the northern part of the basin, the areas highly vulnerable to flooding are Djougou, Copargo, and Pèrèrè. The municipality of Parakou in the northern part of the basin has low vulnerability owing to its very high adaptation capacities. Municipalities in the central-western part of the basin, such as Bante, Savalou, and Dassa Zoume have a medium vulnerability.

When comparing the historical flood vulnerability from observed data (Fig. 5a) with the one obtained from the RCMs (b to g), some similarities appear. The four RCMs indicated the upper north of the basin as vulnerable areas to flood which is in line with the observation if abstraction is made between the difference in two consecutive classes at the exception of Parakou and N_Dali. The difference between classes for these two cities is three which somehow is important. At the central part of the basin, the vulnerability simulated from the RCMs varies slightly with REMO/MPIESM (f) being the closest to the observed vulnerability at the exception of Glazoue with a difference in class of three. At the south of the basin, the RCMs reproduce slightly the observed vulnerability with REMO/MPIESM (f) being the best mainly for the southwestern of the basin. The mean and the median of the four model outputs improve somehow the overall simulations.

Future flood vulnerability

As performed for the historical period, each climate model output was processed using the normalization, aggregation, and classification methods presented above for projected flood vulnerability assessment. The lower box of Fig. 4 displays the change in the median flood vulnerability from the historical to the future period (2020–2050) based on 24 participating members for each of the four RCMs (REMO/MPIESM, RCA4/IPSL, CCLM4/HADGEM2, RACMO/ECEARTH). For most of the climate models, the southern and northern parts of the basin will be more vulnerable to flood by 2050, under the RCP 4.5 (see Figure F3 supplementary material). Only the RCA4/IPSL model predicted: "high vulnerability" for two municipalities (Glazoue and Dassa Zoume) in the center of the basin.

The spatial patterns of change in flood vulnerability vary with the models and there is no clear spatial trend except for the central-western part of the basin where no change was found. Table T2 (see supplementary material) displays the change in flood vulnerability between the future and historical periods for the RCMs' outputs. Decreasing refers to change from upper to lower classes while increasing refers to the opposite. Most of the RCMs indicated no change in future flood vulnerability relative to the historical period taken as reference. The highest decrease in flood vulnerability (29.4%) was simulated from CCLM4/HADGEM2 while the highest increase (41.2%) was obtained from RCA4/IPSL. On average, the RCMs projected a possible decrease in flood vulnerability for 22.1% of the municipalities in the Ouémé Basin, an increase of 27.2%, and no change for 50.7% of the municipality. The very high shift found for some municipalities must be taken with caution considering uncertainties inherent to any modeling and much more to the projection of extreme rainfall (Chen et al. 2013).

Discussions

Methodological scenarios for flood vulnerability assessment

The assessment of flood vulnerability in the ORB explored different methodological approaches. High correlations were obtained among ZC.LA, MM.LA, DT.LA, RA.LA, and RA.GA suggesting that the FVI is not highly sensitive (Tate 2012) to changes in the normalization and aggregation methods except for ZC.GA. The high correlation values found are in line with previous flood vulnerability studies (Yoon 2012; Nazeer and Bork 2019). The divergence of the ZC.GA from other normalization and aggregation approaches through the negative correlation was noted by Moreira et al. (2021) showing that the geometric aggregation does not have the potential to manage information derived from the z-score normalization (Garg et al. 2018).

The average absolute shift in rank position ($\underline{Rs}$) is an adapted tool for testing the robustness, stability, and reliability of the findings (Hudrliková 2013; Nazeer and Bork 2021). $\underline{Rs}$ values of 1.10, 1.13, and 1.19 for the scenarios RA.LA, ZC.LA, and MM.LA respectively are moderate (Merz et al. 2013) implying a moderate deviation from the reference scenario (median ranking). The results are therefore relatively robust to the variation in the initial indicator normalization and aggregation techniques. The ZC.GA scenario indicated the largest difference from the median rank with the highest uncertainty. This probably indicates that the geometric aggregation is not adapted to the Z-score normalization which can be negative for indicator values lower than the average. The geometric aggregation rewards the spatial units with higher scores while linear aggregation favors indicators proportionally to weights (OECD 2005).

The average absolute shift in classes and the Akaike information criterion (AIC) show conjunctly that the equal intervals and natural breaks generally outperformed the other classification methods. This result is consistent with earlier findings (Moreira et al. 2021). However, the high value of AIC mainly for RA.LA and RA.GA reveals high variances in the classes for these scenarios. The quantile classification approach did not rank first for any scenario. As the quantile method divides the data into the equal interval, it may not be appropriate for all types of distribution (Moreira et al. 2021).

Uncertainties in historical and future vulnerabilities

For the historical period, based on the observed data, the southern part of the basin appears to be the most vulnerable to extreme rainfall. This is consistent with previous studies on flood frequency analysis including Hounkpè et al. (2016) and Attogouinon et al. (2017). This work is among the first of its kind to identify flood vulnerability classes for the districts of the Ouémé Basin using a multi-modeling statistical approach.

While the highest vulnerabilities were found for the Southwest of the basin based on observed data, models' outputs for the historical data indicated rather the North. This inconsistency stems from rainfall which is the only difference in terms of inputs for computing observed and modeled (RCMs) vulnerabilities for the historical period. Climate models are less skillful in reproducing extreme rainfall than in reproducing mean rainfall values (Chen et al. 2013). Subsequently, the consideration of the peak over threshold sampling method adopted in this work has resulted in contrasted samples for the observed and models outputs data. Any overestimation or underestimation of rainfall data from the RCMs would propagate in the vulnerability assessment resulting in contrasting results. However, to limit the propagation of this kind of uncertainty, the results were interpreted in relative terms for each RCM rather than absolute values (see Fig. 4). This approach is common in scenario analysis (Huisman et al. 2009; Vaze and Teng 2011; Teng et al. 2012). For example, in an analysis of climate change impact on flood risk at Ebro River Basin (Spain), Lastrada et al. (2020) found important differences in absolute and relative terms for model outputs which they attributed to the uncertainties in climate projections mainly rainfall and downscaling methods.

Changes in flood vulnerability from historical to future periods are RCM dependent. While the outputs of some RCMs projected a decreasing flood vulnerability, others indicated an increase for the same geographical unit. To understand the differences, future extreme rainfall frequency was computed for each RCM (see supplementary material Figure F4). The results were found concordant with the North being the most likely exposed to heavy rainfall, the center highly exposed and the south, the least exposed. Exceptions were found for CCLM4/HADGEM2 for the extreme north and the RCA4/IPSL for the southwest. The degree of similarity of future extreme rainfall frequency of nearly all the RCMs cannot explain the variability of the change in flood vulnerability among the RCMs (lower box of Fig. 4). It was, therefore, hypothesized that the variability may be due to the number of shifts in classes considered as a change. Change in flood vulnerability was recomputed assuming a change effective when there is a minimum of two shifts between the historical and future vulnerability maps (see supplementary material Fig. S2S2). The variability in the change of vulnerability from historical to future periods was substantially reduced. The results found in this case were concordant across RCMs for the North, South, and East of the basin with no change in flood vulnerability. However, RCA4.IPSL indicated an increase in flood vulnerability for four municipalities located in the Southwest. The methodological approach for computing the change in flood vulnerability could substantially influence the outputs.

Some indicators of sensitivity such as population density and land cover vary in time (but also in space), and further quantification of these indicators for the 2020–2050 period should be considered. However, to derive exclusively the impact of future climate, sensitivity indicators were considered constant over time. A possible decrease in future flood vulnerability was found for many districts (22.1%) based on the median of the scenarios. This was essentially due to a possible decrease in heavy rainfall for the future. However, as reported in the literature, projections of rainfall and particularly heavy rainfall in West Africa are subject to many uncertainties (Chen et al. 2013). These results can, however, serve as a proxy for framing adaptation measures and identifying areas where more efforts are required.

Conclusions

The objective of this study was to determine the level of present vulnerability and future vulnerability to flooding risks in the ORB at the Bonou outlet using a multi-modeling statistical approach. The vulnerability assessment was based on the impact chain, which defines vulnerability as resulting from the combination of exposure, sensitivity, and adaptation capacity. Each of the components was developed as indicators that served for computing flood vulnerability index at the municipality scale, used as a basic geographical unit. The methodology applied comprises four indicator normalization methods, two aggregation techniques, four classification methods, and three robustness evaluation approaches.

Among all the classification methods considered in this study, it was found that the equal interval provides the lowest value of the Akaike information criterion (AIC) and thus is the overall best classification method. The lowest AIC was obtained for the min–max normalization with linear aggregation (MM.LA) implying the outperformance of this method over the others. Results also indicate that the ORB is very vulnerable to the adverse impacts of climate change.

For the historical period (1970–2015), the municipalities of Glazoue, Cove, Zagnanado, Agbangnizoun, Toffo, Ze, and Pobè appeared to have a very high vulnerability in the Ouémé Basin. In addition to these municipalities, most areas in the southern part of the basin showed a high vulnerability to pluvial flooding. In the northern part of the basin, the most vulnerable areas to flooding are Djougou, Copargo, and Pèrèrè. For most of the climate models, future vulnerability (2020–2050) will be, to some extent, exacerbated mostly in the southern part of the basin than in the northern part of the basin.

Notwithstanding the challenges related to flood vulnerability assessment as a composite indicator (Mazziotta and Pareto 2013; Nazeer and Bork 2019) for which there is no universally accepted method, the methodology developed here and based on different scenarios reinforce confidence in the results presented. The outcome of this study can provide a solid background to decision-makers for designing appropriate adaptation strategies for the municipalities indicating an increase in flood vulnerability for a minimum of two shifts. However, in the face of the large uncertainties in climate projections, detailed analyses need to be carried out using more climate models (with the possibility of considering sub-daily data) and scenarios to select the bests for framing tailored adaptation measures.

Efforts must focus on strengthening the adaptability of populations through feasible adaptation options that would contribute to strengthening their resilience. Adaptation measures should target either the reduction of the sensitivity or the increase of the adaptive capacity of the system studied. Also, the current study focused on flood vulnerability to extreme rainfall in the study area. Downstream, mainly after the Bonou outlet, flood is mainly due to the river discharge. Therefore, future flood vulnerability studies would target riverine flooding.

Supplementary Information The online version contains supplementary material available at https://doi.org/10.1007/s10113-022-01957-5.

Acknowledgements Comments and suggestions from the Editor and two anonymous reviewers are gratefully acknowledged.

Funding This work was funded by the German Federal Ministry for the Environment, Nature Conservation, and Nuclear Safety (BMU) under the International Climate Initiative through PAS-PNA project (Science-based national adaptation planning in Sub-Saharan Africa). Additional funding was received from DAAD ClimapAfrica program.

References

Akaike H (1974) A new look at the statistical model identification. IEEE Trans Autom Control ac-19:716–723. https://doi.org/10.1109/TAC.1974.1100705

Attogouinon A, Lawin AE, M'Po YN, Houngue R (2017) Extreme precipitation indices trend assessment over the Upper Oueme River Valley-(Benin). Hydrology 4:36. https://doi.org/10.3390/hydrology4030036

Badou DF, Afouda AA, Diekkrüger B, Kapangaziwiri E (2015) Investigation on the 1970s and 1980s drought in four tributaries of the Niger River Basin (West Africa). In: E-proceedings of the 36th IAHR World Congress 28 June – 3 July, 2015, The Hague, the Netherlands. IAHR, pp 1–5. https://researchspace.csir.co.za/dspace/handle/10204/9655. Accessed 12 Dec 2020

Badou DF, Kapangaziwiri E, Diekkrüger B, Hounkpè J, Afouda A (2017) Evaluation of recent hydro-climatic changes in four tributaries of the Niger River Basin (West Africa). Hydrol Sci J 62(5):715–728. https://doi.org/10.1080/02626667.2016.1250898

Balica SF, Wright NG, Meulen van der (2012) A flood vulnerability index for coastal cities and its use in assessing climate change impacts. Nat Hazards https://doi.org/10.1007/s11069-012-0234-1

Behanzin ID, Thiel M, Szarzynski J, Boko M (2016) GIS-based mapping of flood vulnerability and risk in the Bénin Niger River Valley. https://www.weadapt.org/system/files_force/2017/november/idelbert_dagbegnon_ijggs_0.pdf?download=1. Accessed 12 Dec 2020

Birkmann J, Jamshed A, McMillan JM, Feldmeyer D, Totin E et al (2022) Understanding human vulnerability to climate change: A global perspective on index validation for adaptation planning. Science of The Total Environment. https://doi.org/10.1016/j.scitotenv.2021.150065

Bossa A, Diekkrüger B, Agbossou E (2014) Scenario-based impacts of land use and climate change on land and water degradation from the meso to regional scale. Water 6:3152–3181. https://doi.org/10.3390/w6103152

Chen J, Brissette FP, Chaumont D, Braun M (2013) Performance and uncertainty evaluation of empirical downscaling methods in quantifying the climate change impacts on hydrology over two North American river basins. J Hydrol 479:200–214. https://doi.org/10.1016/j.jhydrol.2012.11.062

Coto EB (2002) Flood hazard, vulnerability and risk assessment in the city of Turrialba, Costa Rica. Master Thesis, International Institute for Geo-information Science and Earth Observation

Deng Z (2007) Vegetation dynamics in Oueme Basin, Benin, West Africa. Cuvillier Verlag, 156 p, Göttingen, Germany

Edenhofer O, Madruga RP, Sokona Y, Seyboth K, Kadner S et al (2012) Renewable energy sources and climate change mitigation: special report of the intergovernmental panel on climate change. Cambridge University Press

EM-DAT (2022) The emergency events database - Universite Catholique de Louvain (UCL) - CRED, D. Guha-Sapir, Brussels, Belgium. www.emdat.be. Accessed 25 May 2022

Feizizadeh B, Kienberger S (2017) Spatially explicit sensitivity and uncertainty analysis for multicriteria-based vulnerability assessment. J Environ Plan Manag 60:2013–2035. https://doi.org/10.1080/09640568.2016.1269643

Fritzsche K, Schneiderbauer S, Bubeck P, Kienberger S, Buth M et al (2014) The Vulnerability Sourcebook Concept and guidelines for standardised vulnerability assessments. Deutsche Gesellschaft für Internationale Zusammenarbeit, Bonn and Eschborn, Germany

Füssel HM, Klein RJT (2006) Climate change vulnerability assessments: an evolution of conceptual thinking. Clim Change 75:301–329. https://doi.org/10.1007/s10584-006-0329-3

Garg H, Munir M, Ullah K, Mahmood T, Jan N (2018) Algorithm for T-spherical fuzzy multi-attribute decision making based on improved interactive aggregation operators. Symmetry (Basel) https://doi.org/10.3390/sym10120670

Hauke J, Kossowski T (2011) Comparison of values of Pearson's and Spearman's correlation coefficients on the same sets of data. Quaest Geogr 30:87–93. https://doi.org/10.2478/v10117-011-0021-1
Hebb A, Mortsch L (2007) Floods: mapping vulnerability in the Upper Thames watershed under a changing climate. Project Report XI, University of Waterloo 1–53. http://www.eng.uwo.ca/research/iclr/fids/publications/cfcas-climate/reports/Vulnerability_Mapping_Report.pdf. Accessed 12 Dec 2020
Hempel S, Frieler K, Warszawski L, Schewe J, Piontek F (2013) A trend-preserving bias correction-the ISI-MIP approach. Earth Syst Dyn 4:219–236. https://doi.org/10.5194/esd-4-219-2013
Hounkpè J, Afouda AA, Diekkrüger B, Hountondji F (2015) Modelling extreme streamflows under non-stationary conditions in Ouémé river basin, Benin, West Africa. Hydrological Sciences and Water Security: Past, Present and Future. IAHS (International Association of Hydrological Sciences), Paris, France, pp 143–144. https://doi.org/10.5194/piahs-366-143-2015
Hounkpè J, Diekkrüger B, Afouda AA, Sintondji LOC (2019) Land use change increases flood hazard: a multi - modelling approach to assess change in flood characteristics driven by socio - economic land use change scenarios. Nat Hazards https://doi.org/10.1007/s11069-018-3557-8
Hounkpè J, Diekkrüger B, Badou D, Afouda A (2015b) Non-stationary flood frequency analysis in the Ouémé River Basin, Benin Republic. Hydrology 2:210–229. https://doi.org/10.3390/hydrology2040210
Hounkpè J, Diekkrüger B, Badou DF, Afouda A (2016) Change in heavy rainfall characteristics over the Ouémé River Basin, Benin Republic, West Africa. Climate 4:1–23. https://doi.org/10.3390/cli4010015
Hudrliková L (2013) Composite indicators as a useful tool for international comparison: the Europe 2020 example. Prague Econ Pap 459–473 https://doi.org/10.18267/j.pep.462
Huisman JA, Breuer L, Bormann H, Bronstert A, Croke BFW et al (2009) Assessing the impact of land use change on hydrology by ensemble modeling (LUCHEM) III: Scenario analysis. Adv Water Resour 32:159–170. https://doi.org/10.1016/j.advwatres.2008.06.009
INSAE (2015) Institut National de Statistiques et de l'Analyse Economique. Tendances de la pauvreté au Bénin 2007–2015. Cotonou, Bénin. http://insae.bj. Accessed 12 Accessed 2020
Kumpulainen S (2006) Vulnerability concepts in hazard and risk assessment. Special Paper-Geological Survey of Finland 42:65–74
Lastrada E, Cobos G, Torrijo FJ (2020). Analysis of climate change's effect on flood risk. Case Study of Reinosa in the Ebro River Basin. Water 12(4):1114 https://doi.org/10.3390/w12041114
Lebel T, Ali A (2009) Recent trends in the Central and Western Sahel rainfall regime (1990–2007). J Hydrol 375:52–64. https://doi.org/10.1016/j.jhydrol.2008.11.030
Lung T, Lavalle C, Hiederer R, Dosio A, Bouwer L (2013) A multi-hazard regional level impact assessment for Europe combining indicators of climatic and non-climatic change. Glob Environ Chang 23:522–536. https://doi.org/10.1016/j.gloenvcha.2012.11.009
Mazari M, Tirado C, Nazarian S, Aldouri R (2017) Impact of geospatial classification method on interpretation of intelligent compaction data. Transp Res Rec 2657:37–46. https://doi.org/10.3141/2657-05
Mazziotta M, Pareto A (2013) Methods for constructing composite indicators: one for all or all for one. Ital J Econ Demogr Stat 67(2):67–80. https://www.istat.it/it/files/2013/12/Rivista2013_Mazziotta_Pareto.pdf. Accessed 12 Dec 2020
MEHU (2011) Ministère de l'Environnement de l'Habitat et de l'Urbanisme. Deuxieme communication nationale de la République du Bénin sur les changements climatiques. Cotonou, Bénin. https://unfccc.int/resource/docs/natc/bennc2f.pdf. Accessed 12 Accessed 2020
Merz M, Hiete M, Comes T, Schultmann F (2013) A composite indicator model to assess natural disaster risks in industry on a spatial level. J Risk Res 16:1077–1099. https://doi.org/10.1080/13669877.2012.737820
Moreira LL, de Brito MM, Kobiyama M (2021) Effects of different normalization, aggregation, and classification methods on the construction of flood vulnerability indexes. Water 13:98. https://doi.org/10.3390/w13010098
N'Tcha M'Po Y, Lawin E, Yao B, Oyerinde G, Attogouinon A et al (2017) Decreasing past and mid-century rainfall indices over the Ouémé River Basin, Benin (West Africa). Climate 5:74. https://doi.org/10.3390/cli5030074
Nazeer M, Bork HR (2019) Flood vulnerability assessment through different methodological approaches in the context of North-West Khyber Pakhtunkhwa. Pakistan Sustainability 11(23):6695. https://doi.org/10.3390/su11236695
Nazeer M, Bork HR (2021) A local scale flood vulnerability assessment in the flood-prone area of Khyber Pakhtunkhwa, Pakistan. Nat Hazards 105:755–781. https://doi.org/10.1007/s11069-020-04336-7
Nicholson ES (2001) Climatic and environmental change in Africa during the last two centuries. Clim Res 17:123–144. https://doi.org/10.3354/cr017123
Nkrumah F, Vischel T, Panthou G, Klutse NA, Adukpo D et al (2019) Recent trends in the daily rainfall regime in Southern West Africa. Atmosphere (basel) 10:1–15. https://doi.org/10.3390/ATMOS10120741
OECD (2005) Handbook on constructing composite indicators: methodology and user guide. https://www.oecd.org/sdd/42495745.pdf. Accessed 12 Accessed 2020
Parry M, Canziani O, Palutikof J, van der Linden P, Hanson C (2007) Bilan 2007 des changements climatiques Conséquences, adaptation et vulnérabilité Résumé à l'intention des décideurs. https://www.ipcc.ch/site/assets/uploads/2020/02/ar4-wg2-sum-vol-fr.pdf. Accessed 12 Dec 2020
Ritzsche K, Schneiderbauer S, Bubeck P, Kienberger S, Buth M et al (2015) Guide de référence sur la vulnérabilité: Annexe. https://www.adaptationcommunity.net/download/va/vulnerability-guides-manualsreports/Guide_de_reference_sur_la_vulnerabilite__Annexe_-_GIZ_2014.pdf . Accessed 12 Dec 2020
Saisana M, Saltelli A, Tarantola S (2005) Uncertainty and sensitivity analysis techniques as tools for the quality assessment of composite indicators. J R Stat Soc Ser A Stat Soc 168:307–323. https://doi.org/10.1111/j.1467-985X.2005.00350.x
SAP-Benin (2015) Determination des seuils et niveaux d'alerte relatifs au risque d'inondationpluviale au Benin. Rapport
Solomon S, Manning M, Marquis M, Qin D, Climate Change (2007) The physical science basis: Working group I contribution to the fourth assessment report of the IPCC. Cambridge University Press, 2007 Sep 10
Spearman C (1904) The proof and measurement of association between two things. Am J Psychol 15:72–101. https://doi.org/10.1037/h0065390
Sultan B, Gaetani M (2016) Agriculture in West Africa in the twenty-first century: climate change and impacts scenarios, and potential for adaptation. Front Plant Sci https://doi.org/10.3389/fpls.2016.01262
Tate E (2012) Social vulnerability indices: a comparative assessment using uncertainty and sensitivity analysis. Nat Hazards 63:325–347. https://doi.org/10.1007/s11069-012-0152-2
Tazen F, Diarra A, Kabore RFW, Ibrahim B, Bologo/Traoré M et al (2019) Trends in flood events and their relationship to extreme rainfall in an urban area of Sahelian West Africa: The case study

of Ouagadougou, Burkina Faso. J Flood Risk Manag https://doi.org/10.1111/jfr3.12507

Teng J, Chiew FHS, Timbal B, Wang Y, Vaze J et al (2012) Assessment of an analogue downscaling method for modelling climate change impacts on runoff. J Hydrol 472–473:111–125. https://doi.org/10.1016/j.jhydrol.2012.09.024

Tóth S (2008) Vulnerability Analysis in the Körös-corner flood area along the Middle-Tisza River. http://resolver.tudelft.nl/uuid:b813a25e-9675-4329-8a7f-35b6bbe0cbc4, Accessed 12 Dec 2020

Vaze J, Teng J (2011) Future climate and runoff projections across New South Wales, Australia: results and practical applications. Hydrol Process 25:18–35. https://doi.org/10.1002/hyp.7812

Villordon BB (2012) Community-based flood vulnerability index for urban flooding: understanding social vulnerabilities and risks. Université de Nice-Sophia Antipolis. https://www.theses.fr/2014NICE4145.pdf. Accessed 12 Dec 2020

World Bank (2011) Inondation au Benin: Rapport d'évaluation des Besoins Post Catastrophe. Cotonou, Benin, 84 p. https://www.gfdrr.org/sites/default/files/publication/pda-2011-benin-fr.pdf

Yoon DK (2012) Assessment of social vulnerability to natural disasters: a comparative study. Nat Hazards 63:823–843. https://doi.org/10.1007/s11069-012-0189-2